

Identification of a *Rhodobacter capsulatus* L-Cysteine Desulfurase That Sulfurates the Molybdenum Cofactor When Bound to XdhC and before Its Insertion into Xanthine Dehydrogenase[†]

Meina Neumann,[‡] Walter Stöcklein,[§] Anne Walburger,^{||} Axel Magalon,^{||} and Silke Leimkühler^{*,‡}

Departments of Proteinanalytics and Analytical Biochemistry, Institute of Biochemistry and Biology, University of Potsdam, 14476 Potsdam, Germany, and Laboratoire de Chimie Bactérienne, Institut Biologie Structurale et Microbiologie, CNRS, 31 Chemin Joseph Aiguier, 13402 Marseille Cedex 09, France

Received April 3, 2007; Revised Manuscript Received May 9, 2007

ABSTRACT: The molybdenum cofactor (Moco) containing enzymes aldehyde oxidase and xanthine dehydrogenase (XDH) require for activity a sulfuration step that inserts a terminal sulfur ligand into Moco. XdhC was shown to be essential for the production of active XDH in *Rhodobacter capsulatus* but is itself not a subunit of the purified enzyme. XdhC binds stoichiometric amounts of Moco and is further able to transfer its bound Moco to XDH. Previous work suggested that XdhC particularly stabilizes the sulfurated form of Moco before the insertion into XDH. In this work, we identify an *R. capsulatus* L-cysteine desulfurase, NifS4, which is involved in the formation of the Mo=S ligand of Moco. We show that NifS4 interacts with XdhC and not with XDH. NifS4 mobilizes sulfur from L-cysteine by formation of a protein-bound persulfide intermediate and transfers this sulfur further to Moco. This reaction was shown to be more effective than the chemical sulfuration of Moco using sulfide as sulfur source. Further studies clearly showed that Moco is sulfurated before the insertion into XDH, while it is bound to XdhC. Conclusively, XdhC has a versatile role in *R. capsulatus*: binding of Moco, interaction with NifS4 for the sulfuration of Moco, protection of sulfurated Moco from oxidation, and further transfer to XDH.

Xanthine dehydrogenase (XDH,¹ EC 1.17.1.4) is a complex molybdo/iron–sulfur flavoenzyme that belongs to the xanthine oxidase family of molybdoenzymes (1). The enzyme catalyzes the hydroxylation of hypoxanthine to xanthine and xanthine to uric acid, with the concomitant reduction of NAD⁺ to NADH. A water molecule is used as the ultimate source of oxygen incorporated into the product (2). XDH is present in a broad range of eukaryotic and prokaryotic organisms, with the enzymes isolated from bovine milk and *Rhodobacter capsulatus* being structurally and functionally best characterized (3, 4). *R. capsulatus* XDH is composed of two subunits, XdhA and XdhB, which form an ($\alpha\beta$)₂ heterodimer, containing a flavin adenine dinucleotide (FAD), two nonidentical [2Fe-2S] clusters bound to the XdhA subunit, and a molybdenum cofactor (Moco) bound to the XdhB subunit (4). For all members of the

xanthine oxidase family the sulfurated form of Moco is essential for catalysis, where the equatorial of the two oxygen ligands is exchanged by sulfur. This Mo=S sulfur was shown by Gutteridge et al. (5) to be the cyanolyzable sulfur identified by Massey and Edmondson (6).

In *R. capsulatus*, mutational analysis identified a third gene that is cotranscribed with *xdhA* and *xdhB*, which has been designated *xdhC* (7). The gene product of *xdhC* is essential for XDH activity; however, XdhC is not a subunit of active XDH (4, 7). XDH purified from an *R. capsulatus xdhC* strain consists of an ($\alpha\beta$)₂ heterodimer with a full complement of iron–sulfur clusters and FAD but no inserted Moco or molybdopterin (MPT) (7). A system for heterologous expression of *R. capsulatus xdhABC* in *Escherichia coli* has been reported (8, 9), enabling the purification of active XDH with a full complement of Moco harboring the equatorial Mo=S ligand. Analysis of the requirement of *xdhC* during heterologous expression of XDH in *E. coli* cells showed that XdhC is required to produce active XDH, especially under increased oxygen supply (10). In the absence of XdhC, inactive XDH contained Moco, but the terminal sulfur ligand required for activity was missing. The strong influence of oxygen supply suggested a role of XdhC in protecting the exchange of the sulfur ligand of Moco against an oxygen atom. XdhC was shown to bind stoichiometric amounts of Moco and is further able to transfer its bound Moco to Moco-free apo-XDH by a specific interaction with the XdhB subunit. Previous work suggested that XdhC particularly stabilizes the sulfurated form of Moco before the insertion

[†] This work was supported by Deutsche Forschungsgemeinschaft Grant LE1171/3-3 (to S.L.) and the Fonds der Chemischen Industrie (FCI).

* To whom correspondence should be addressed: tel, +49-331-977-5603; fax, +49-331-977-5419; e-mail, sleim@uni-potsdam.de.

[‡] Department of Proteinanalytics, University of Potsdam.

[§] Department of Analytical Biochemistry, University of Potsdam.

^{||} Laboratoire de Chimie Bactérienne, CNRS.

¹ Abbreviations: XDH, xanthine dehydrogenase; FAD, flavin adenine dinucleotide; MPT, molybdopterin; Moco, molybdenum cofactor; AO, aldehyde oxidase; PLP, pyridoxal 5'-phosphate; SPR, surface plasmon resonance; hSO, human sulfite oxidase; PCR, polymerase chain reaction; NTA, nitrilotriacetic acid; TED, tris(carboxymethyl)ethyl-enediamine; MU, Miller units; RU, resonance units; bis-MGD, bismolybdopterin guanine dinucleotide cofactor; TMAO, trimethylamine N-oxide.

Table 1: *E. coli* Strains and Plasmids Used in This Work

	description	ref or source
strain or plasmid		
BL21(DE3)	F ⁻ <i>ompT hsdDB</i> (r _B ⁻ m _B ⁻) <i>gal dcm</i> (DE3)	Novagen
ER2566(DE3)	F ⁻ λ - <i>fhuA2 [lon] ompT lacZ::T7 gene1 gal sulA11 D(mcrC-mrr)114::IS10 R(mcr-73::miniTn10--TetS)2 R(zgb-210::Tn10) (TetS), endA1 [dcm]</i>	New England Biolabs
RK5200	RK4353 <i>chlA::Mu cts [moaA-]</i>	23
TP1000	MC4100 Δ (<i>mobAB</i>)	24
BHT101	F ⁺ , <i>cya-99, araD139, galE15, galK16, rpsL1(Str^R), hsdR2, mcrA1, mcrB1</i>	25
BHT101 <i>moa</i>	BHT101 <i>moa254::Tn10</i>	26
expression vectors		
pTG818	pTrcHis based expression vector for the His-tagged Moco domain of hSO	24
pSL207	pTrcHis based expression vector for XDH	8
pAK20	pTYB2 based expression vector for intein-tagged XdhC	10
pET28a	T7 RNA polymerase based expression vector, Km ^R	Novagen
pMN19	pET28a, His-tagged NifS2, <i>NdeI</i> – <i>SalI</i>	this work
pMN20	pET28a, His-tagged NifS4, <i>NdeI</i> – <i>XhoI</i>	this work
pMN51	pET28a, His-tagged NifS3, <i>NheI</i> – <i>XhoI</i>	this work
pMN52	pET28a, His-tagged NifS2- Δ 1–188, <i>NdeI</i> – <i>SalI</i>	this work
two-hybrid vectors		
pT18-zip	pUC19 derivative, leucine zipper fused to T18 fragment of Cya, Amp ^R	29
pT25-zip	pACYC184 derivative, leucine zipper fused to T25 fragment of Cya, Cm ^R	29
pMN49	pT18, NifS2-T18 fusion protein, <i>KpnI</i> – <i>KpnI</i>	this work
pMN42	pT18, NifS3-T18 fusion protein, <i>KpnI</i> – <i>KpnI</i>	this work
pMN33	pT18, NifS4-T18 fusion protein, <i>KpnI</i> – <i>KpnI</i>	this work
pMN39	pT18, XdhC-T18 fusion protein, <i>KpnI</i> – <i>KpnI</i>	this work
pMN45	pT18, XdhAB-T18 fusion protein, <i>KpnI</i> – <i>KpnI</i>	this work
pMN48	pT25, T25-NifS2 fusion protein, <i>KpnI</i> – <i>KpnI</i>	this work
pMN47	pT25, T25-NifS3 fusion protein, <i>KpnI</i> – <i>KpnI</i>	this work
pMN35	pT25, T25-NifS4 fusion protein, <i>KpnI</i> – <i>KpnI</i>	this work
pMN34	pT25, T25-XdhC fusion protein, <i>KpnI</i> – <i>KpnI</i>	this work
pMN43	pT25, T25-XdhAB fusion protein, <i>KpnI</i> – <i>KpnI</i>	this work

into XDH (10). In prokaryotes, a specific protein involved in the insertion of the Mo=S ligand of Moco has not been identified to date.

In contrast, proteins with a specific Moco sulfurase activity were identified in a number of eukaryotes. The first report was given by Wahl et al. (11) describing a mutation in the *Drosophila melanogaster* maroon-like locus (*ma-l*) which impaired the activity of XDH and aldehyde oxidase (AO), while the activity of sulfite oxidase remained unaffected. Since it was possible to reconstitute XDH and AO activity by the addition of dithionite and sulfide to *ma-l* extracts, they concluded that a gene coding for a Moco sulfurase was mutated in *ma-l* flies (11), which was cloned and characterized in further studies (12). Proteins with homologies to *D. melanogaster* MA-L were also identified in humans [HMCS (13)], cattle [MCSU (14)], fungi [HxB (12, 15)], and plants [ABA3 (16)]. Eukaryotic Moco sulfurases are two-domain proteins with an N-terminal domain showing homologies to bacterial L-cysteine desulfurases (E.C. 2.1.8.7) of the NifS family and a C-terminal domain of unknown function. The currently best characterized Moco sulfurase is ABA3 from *Arabidopsis thaliana* (17). Recombinant ABA3 was used for in vitro sulfuration of the Moco site of purified *A. thaliana* AO, showing that the conserved Cys430 residue in the N-terminal NifS-like domain is involved in this reaction (18). The C-terminal domain of ABA3 lacks homologies to other functionally described proteins in eukaryotes but contains an annotated [2Fe-2S] binding site (19).

In general, L-cysteine desulfurases are homodimeric proteins that utilize pyridoxal 5'-phosphate (PLP) to catalyze the reductive elimination of sulfur from L-cysteine, resulting in the formation of alanine and an enzyme-bound cysteine–persulfide intermediate (20). Due to sequence differences in the persulfuration site, L-cysteine desulfurases are classified

into group I members (e.g., IscS from *E. coli*) and group II members (e.g., CsdB and CsdA from *E. coli*) of the NifS family (21). DNA analysis revealed that *R. capsulatus* contains four coding regions with homologies to L-cysteine desulfurases. One of them, encoded by the *nifS* gene, is located in the nitrogenase operon and is essential for activity of the MoFe nitrogenase (22). The specific role of NifS for the synthesis of FeMoco for nitrogenase made it likely that one of the three remaining NifS-like proteins catalyzes the L-cysteine desulfurase reaction required for XDH activity.

This report describes the identification of a specific *R. capsulatus* NifS-like protein involved in the formation of the sulfurated form of Moco bound to XdhC. In vivo interaction studies between XdhC and the *R. capsulatus* L-cysteine desulfurases NifS2, NifS3, and NifS4 were performed, using an *E. coli* two-hybrid system. In addition, we purified and characterized the three L-cysteine desulfurases after heterologous expression in *E. coli* and carried out surface plasmon resonance (SPR) experiments. In vivo and in vitro interaction studies identify NifS4, a class II member of L-cysteine desulfurases, as the tightest interactant of XdhC. Moreover, the sulfuration reaction mediated by the L-cysteine desulfurase is significantly higher when Moco is bound to XdhC rather than XDH. These results show that *R. capsulatus* NifS4 acts as a Moco sulfurase which in conjunction with XdhC sulfurates Moco before its insertion into XDH.

EXPERIMENTAL PROCEDURES

Bacterial Strains, Plasmids, Media, and Growth Conditions. The bacterial strains and plasmids used in this work are listed in Table 1. *E. coli* BL21(DE3) cells were used for expression of the *R. capsulatus* L-cysteine desulfurases NifS2,

NifS3, and NifS4. XdhC was expressed in *E. coli* ER2566- (DE3) and purified as described previously (10). Moco-free apo-XDH was obtained after expression in *E. coli* RK5200 (23) and was purified as described by Neumann et al. (10). The Moco domain of human sulfite oxidase (hSO) was expressed in *E. coli* TP1000 cells and purified after the report of Temple et al. (24). For *E. coli* two-hybrid analyses *E. coli* BHT101 and its derivative BHT101moa were used (25, 26). Bacterial cultures were generally grown in LB medium under aerobic conditions at 30 °C. When required, 1 mM sodium molybdate, 150 µg/mL ampicillin, 50 µg/mL chloramphenicol, or 25 µg/mL kanamycin was added to the medium. For *E. coli* two-hybrid assays, the LB medium was supplemented with 100 µg/mL ampicillin, 50 µg/mL chloramphenicol, and 50 µM IPTG, and cultures were grown without agitation.

Cloning, Expression, and Purification of NifS2, NifS2Δ1–188, NifS3, and NifS4. DNA sequences of the *R. capsulatus* L-cysteine desulfurases were obtained from the ERGO database with the accession numbers RRC01303, RRC01538, and RRC01545 (www.ergo-light.com). The DNA fragments containing the coding regions for *R. capsulatus* nifS2, nifS3, and nifS4 were amplified by polymerase chain reaction (PCR), and flanking restriction sites were introduced. *nifS2* and *nifS2-Δ1–188* were cloned into the *NdeI*–*SalI* sites, *nifS3* into the *NheI*–*XhoI* sites, and *nifS4* into the *NdeI*–*XhoI* sites of pET28a (Novagen), resulting in plasmids pMN19, pMN20, pMN51, and pMN52, respectively.

For expression of NifS2, NifS2-Δ1–188, and NifS3, *E. coli* BL21(DE3) cells were transformed with the plasmids pMN19, pMN20, and pMN52, respectively. One liter of LB was inoculated with 10 mL of an overnight culture and incubated at 30 °C until an OD_{600nm} of 0.3–0.5. The expression was induced with 100 µM IPTG and harvested after 5 h. The pellet was resuspended in phosphate buffer (50 mM NaH₂PO₄, 300 mM NaCl, pH 8.0). The cells were lysed by several passages through a French pressure cell, and the cleared lysate was applied to 1 mL of Ni-nitrilotriacetate (NTA; Qiagen) resin per liter of cell culture. The column was washed with 20 column volumes of each phosphate buffer containing 10 or 20 mM imidazole. The protein was eluted with buffer containing 250 mM imidazole and dialyzed against 100 mM Tris, pH 7.2 (pH 7.4 for NifS2-Δ1–188).

For the expression of NifS3, *E. coli* BL21(DE3) was transformed with plasmid pMN51, and 1 L of LB supplemented with 20 µM IPTG was inoculated with 2 mL of an overnight culture and incubated at 30 °C for 22 h. The cells were harvested and resuspended in phosphate buffer. The cells were lysed by several passages through a French pressure cell, and the cleared lysate was applied to 0.2 mL of Ni-tris(carboxymethyl)ethylenediamine (TED; Macherey & Nagel) resin per liter of culture. The column was washed with 40 column volumes of phosphate buffer containing 10 mM imidazole. The protein was eluted with the same buffer containing 250 mM imidazole and dialyzed against 100 mM Tris, pH 7.2.

Enzyme Assays. XDH activity was assayed following NAD⁺ reduction at 340 nm as described previously (10). XDH activities obtained were compared to the *k*_{cat} of wild-type XDH reported previously (9), and for comparison, this value was set to 100% activity. Apparent *k*_{cat} values for

L-cysteine desulfurase activities were determined with varying concentrations of L-cysteine by estimating the initial rate of hydrogen sulfide production quantified as methylene blue using the assay parameters described by Zheng et al. (27) and Urbina et al. (28). Assay mixtures in a total volume of 0.8 mL contained 25 mM Tris, 100 mM NaCl, 125 µM DTT (pH 7.4), and either 8 nmol of NifS2-Δ1–188, 40 nmol of NifS3, or 40 nmol of NifS4. The reactions were initiated by addition of L-cysteine (20–200 µM) and incubated for 10 min at 30 °C before the reactions were stopped by addition of 100 µL of 20 mM *N,N*-dimethyl-*p*-phenylenediamine in 7.2 M HCl. One hundred microliters of 30 mM FeCl₃ in 1.2 M HCl was added, and methylene blue was determined at 670 nm after an incubation time of 20 min. The standard curve was recorded with sodium sulfide as sulfur source.

Moco/MPT Analysis. The Moco or MPT content of purified XDH was quantified after conversion to Form A as described previously (10).

***E. coli* Two-Hybrid Assays.** For the construction of C- and N-terminal adenylate cyclase fusions, the *R. capsulatus* *xdhC*, *nifS2*, *nifS3*, and *nifS4* genes were amplified by PCR and cloned into the *KpnI* sites of vectors pT25-*zip* and pT18-*zip*, respectively (29). BHT101 and BHT101moa strains were cotransformed with the pT18- and pT25-based plasmids listed in Table 1 and incubated overnight at 30 °C in LB medium supplemented with 50 µM IPTG. β-Galactosidase activity was assayed as described by Magalon et al. (26) and expressed in Miller units (MU) (30). Plasmids containing a leucine zipper encoding counterpart were used as negative controls.

Surface Plasmon Resonance Measurements. Binding experiments were performed with the SPR-based instrument Biacore 2000 on CM5 sensor chips at a temperature of 25 °C and a flow rate of 10 µL/min, using the control software 2.1 and evaluation software 3.0 (Biacore AB, Uppsala, Sweden). XdhC and bovine serum albumin were immobilized via amine coupling at 570–650 resonance units (RU) per flow cell. Briefly, flow cells were activated with a mixture containing 200 mM *N*-(3-dimethylaminopropyl)-*N'*-ethylcarbodiimide hydrochloride (EDC) and 50 mM *N*-hydroxysuccinimide (NHS) for 7 min. Proteins were injected for 5 min at 20 µg/mL in 10 mM acetate, pH 5 (XDH) or 4 (BSA). The running buffer contained 10 mM Hepes, 150 mM NaCl, 3.4 mM EDTA, and 0.005% Tween-20, pH 7.4. The flow cells were regenerated by injection of 20 mM HCl. The successful, native immobilization of XdhC was validated by the binding of XDH (10). As a control, the sensorgrams obtained with the bovine serum albumin were subtracted from the ones obtained with immobilized XdhC.

In Vitro Sulfuration. In vitro sulfuration was carried out anaerobically using a Coy anaerobic chamber (Coy Laboratory Products Inc.). Three hundred fifty microliters of 100 µM L-cysteine desulfurases was preincubated with 50 µL of 1 M L-cysteine at 4 °C for 10 min before an excess of L-cysteine was removed by gel filtration using Nick columns (GE Healthcare). The persulfuration rate of 100 µL of each L-cysteine desulfurase (70 µM) was determined by the production of methylene blue as described above. Free Moco was obtained by denaturation of Moco-hSO as described previously (10). Moco sulfuration by different L-cysteine desulfurases was determined in mixtures containing 20 µM L-cysteine desulfurase, 100 µM sodium dithionite, 2 µM

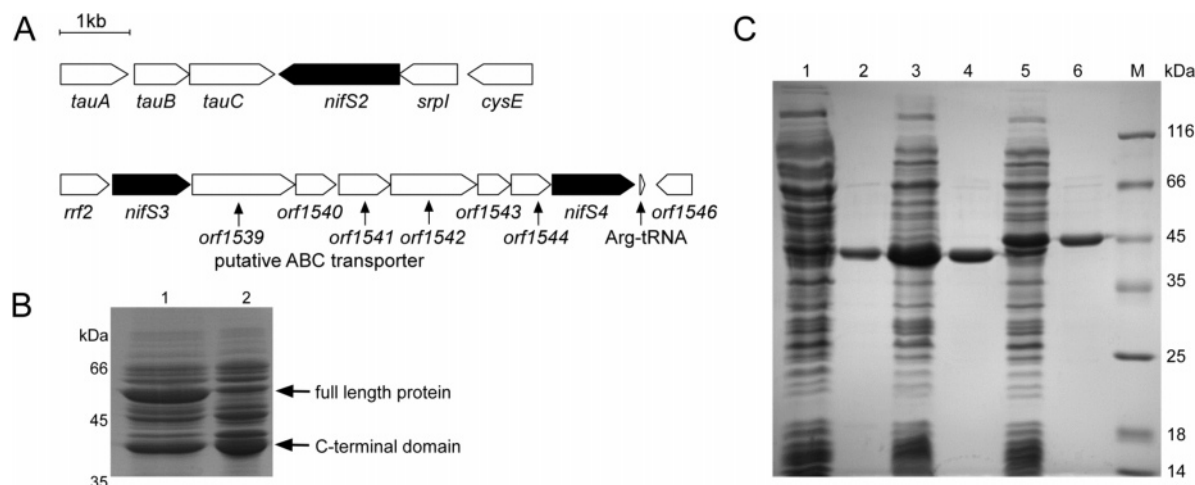


FIGURE 1: Genomic organization of *R. capsulatus* L-cysteine desulfurases and purification of NifS2, NifS3, and NifS4 after heterologous expression in *E. coli*. (A) The localization of genes and open reading frames are given by horizontal arrows carrying their respective gene designations. Black horizontal arrows emphasize the conserved genes coding for L-cysteine desulfurases NifS2, NifS3, and NifS4 in *R. capsulatus*. (B) 12% SDS-PAGE of NifS2 after Ni-NTA chromatography: lane 1, 5 μ L of protein eluted after Ni-NTA chromatography; lane 2, 5 μ L of protein after dialysis overnight against 100 mM Tris, pH 7.2. (C) 12% SDS-PAGE of purification stages of NifS2-Δ1-188, NifS3, and NifS4: lane 1, 1 μ L of *E. coli* BL21(DE3)xpMN52 extract after cell lysis; lane 2, 4 μ g of NifS2-Δ1-188 after Ni-NTA chromatography; lane 3, 1 μ L of *E. coli* BL21(DE3)xpMN51 extract after cell lysis; lane 4, 5 μ g of NifS3 after Ni-TED chromatography; lane 5, 1 μ L of *E. coli* BL21(DE3)xpMN20 extract after cell lysis; lane 6, 4 μ g of NifS4 after Ni-NTA chromatography.

XdhC, and 45 μ M Moco and incubation for 1 h at 4 $^{\circ}$ C in a total volume of 350 μ L of 100 mM Tris (pH 7.2). Fifty microliters of 5 μ M apo-XDH was subsequently added, and the mixtures were incubated for additional 2 h before XDH activity was determined. As controls, samples without XdhC addition were used. For determination of the background sulfuration by dithionite, samples were incubated without L-cysteine desulfurase. Chemical sulfuration was tested by addition of 75 μ M sodium sulfide. For each experiment independently purified XdhC was used.

For comparison of the sulfuration of Moco before and after insertion into apo-XDH, the ratio of Moco to XdhC was changed to excess XdhC to ensure the complete binding of Moco. Moco was sulfurated before insertion into apo-XDH by incubation of 11.6 μ M NifS4, 4 μ M dithionite, 2 μ M Moco, and 10 μ M XdhC for 1 h at 4 $^{\circ}$ C. One micromolar apo-XDH was added afterward to a total volume of 600 μ L of 100 mM Tris (pH 7.2), and samples were incubated for 2 h. As control, a mixture without XdhC addition was used. Free Moco was inserted into XDH and sulfurated by incubation of 1 μ M apo-XDH with 2 μ M Moco and 4 μ M sodium dithionite for 1 h. Either 11.6 μ M NifS4 or 10 μ M sodium sulfide was added to a total volume of 600 μ L of 100 mM Tris, pH 7.2, and samples were incubated additionally for 2 h. Four hundred microliters of each sample was used to determine the MPT/Moco content, and 100 μ L of the samples were assayed for XDH activity.

RESULTS

Genomic Organization of Genes Coding for L-Cysteine Desulfurases in *R. capsulatus*. While Moco sulfurases were identified in a number of eukaryotes, a specific protein involved in the sulfuration of Moco remained yet unknown in prokaryotes. Since the N-terminus of Moco sulfurases shows amino acid sequence homologies to L-cysteine desulfurases, we suggested that a separate NifS-like protein is involved in this reaction in *R. capsulatus*. Four genes coding for L-cysteine desulfurases were identified in the *R. capsu-*

latus genome, designated *nifS* (22), *nifS2* (31), *nifS3*, and *nifS4* (Figure 1A). Amino acid sequence alignment revealed that NifS3 belongs to class I of L-cysteine desulfurases, showing a sequence identity of 28% to *E. coli* IscS. NifS2 and NifS4 both belong to class II of L-cysteine desulfurases, showing sequence identities in the range of 47–49% to *E. coli* CsdB. In total, NifS2, NifS3, and NifS4 share only few sequence identities among each other, with 12% identity between NifS2 and NifS3, 17% identity between NifS3 and NifS4, and 30% identity between NifS2 and NifS4 (Figure S1; see Supporting Information).

R. capsulatus nifS mutants showed a specific phenotype for MoFe nitrogenase with no influence on XDH activity (22, 32), while NifS3 and NifS4 appear to be essential for the viability of *R. capsulatus*, since the construction of interposon mutants were so far not successful.² The role of the putative ABC transporter located in between *nifS3* and *nifS4* is currently unknown. Additional studies on NifS2 and the taurine transporter (*tauABC*) located directly downstream of *nifS2*, which is transcribed in the opposite direction, showed that expression of *R. capsulatus tauABC* and *nifS2* is inhibited by sulfate, suggesting that the genes might belong to the same regulon (31). Genomic analysis suggested that *nifS2* is cotranscribed with *srpI* and *cysE*, a serine acetyltransferase involved in cysteine metabolism (31). However, interposon mutants of *nifS2* did not give rise to a specific phenotype with respect to xanthine utilization.²

Heterologous Expression, Purification, and Characterization of Three *R. capsulatus* L-Cysteine Desulfurases. Since interposon mutants in the genes coding for L-cysteine desulfurases in *R. capsulatus* were apparently either lethal or did not show any effect on xanthine utilization, we purified and characterized the three remaining proteins with homologies to the specific NifS protein for MoFe nitrogenase. For purification of NifS2, NifS3, and NifS4, fusion proteins were generated, each containing an N-terminal His₆ tag for metal

² B. Masepohl, unpublished data.

Table 2: Spectrophotometric and Kinetic Characteristics of the L-Cysteine Desulfurases

	NifS family group ^a	absorption maximum ^b (nm)	K_M (cysteine) ^c (μ M)	k_{cat} (cysteine) ^c (min^{-1})
NifS2	II	425	ND ^d	ND
NifS2- Δ 1–188	II	424	53 ± 3	8.4 ± 0.1
NifS3	I	415	94 ± 7	5.0 ± 0.1
NifS4	II	421	130 ± 18	4.1 ± 0.2

^a Classification by homology to *E. coli* L-cysteine desulfurases as described by Mihara et al. (21). ^b Second peak beside the 280 nm peak of each L-cysteine desulfurase based on absorption of PLP. ^c Kinetic parameters determined as apparent values by quantification of formed methylene blue at varying cysteine concentrations after the procedure described by Urbina et al. (28). ^d ND, none determined.

affinity chromatography purification (Experimental Procedures). Amino acid sequence analysis showed that NifS2 contains an N-terminal extension of 188 amino acids in comparison to other L-cysteine desulfurases, which did not show any similarities to proteins of known function in the database. As shown in Figure 1B, this N-terminal extension is cleaved rapidly from the holoprotein during affinity purification by Ni-NTA. The remaining C-terminal part had a size of 40 kDa (Figure 1B), and analysis by MALDI/TOF mass spectrometry showed that the cleavage site is located after amino acid 188 of NifS2 (data not shown). The instability allowed no purification of the complete protein. On the basis of these results an N-terminal deletion mutant of NifS2 was constructed containing a deletion of amino acids 1–188 (NifS2- Δ 1–188). After heterologous expression in *E. coli*, the soluble fractions of NifS2- Δ 1–188, NifS3, and NifS4 were purified by affinity chromatography (Experimental Procedures). After elution one major band was displayed for each protein on Coomassie brilliant blue R-stained SDS–polyacrylamide gels with sizes of 43, 42, and 46 kDa (Figure 1C). This procedure yielded about 20 mg of protein/L of *E. coli* culture for NifS2- Δ 1–188, 0.4 mg/L of *E. coli* culture for NifS3, and 19 mg/L of *E. coli* culture for NifS4. The elution profiles of NifS2- Δ 1–188, NifS3, and NifS4 from a size exclusion column revealed that each protein existed as a dimer in solution (data not shown).

The purified L-cysteine desulfurases were also characterized by UV–vis spectroscopy. Each protein showed a characteristic PLP peak between 415 and 425 nm, which could be reduced by the addition of 10 mM L-cysteine (Table 2). To determine the kinetic constants of each L-cysteine desulfurase, steady-state kinetics were performed with L-cysteine using the assay described by Urbina et al. (28). Apparent K_M and k_{cat} values were determined for each L-cysteine desulfurase and are listed in Table 2. NifS2- Δ 1–188 showed both the lowest K_M value of $53 \pm 3 \mu\text{M}$ and the highest turnover number of $8.4 \pm 0.1 \text{ min}^{-1}$. This K_M is very close to the apparent K_M obtained for *A. thaliana* ABA3 of $50 \mu\text{M}$ (18). In comparison, NifS3 had a lower turnover number of $5.0 \pm 0.1 \text{ min}^{-1}$ but a significantly higher K_M value of $94 \pm 7 \mu\text{M}$. NifS4 showed the lowest turnover number of the three proteins of $4.1 \pm 0.2 \text{ min}^{-1}$ and the highest K_M value of $130 \pm 18 \mu\text{M}$ (Table 2).

Analysis of Protein–Protein Interactions Using the *E. coli* Two-Hybrid System and Surface Plasmon Resonance Measurements. Protein–protein interactions play a major role in biological networks. In previous work, we showed that

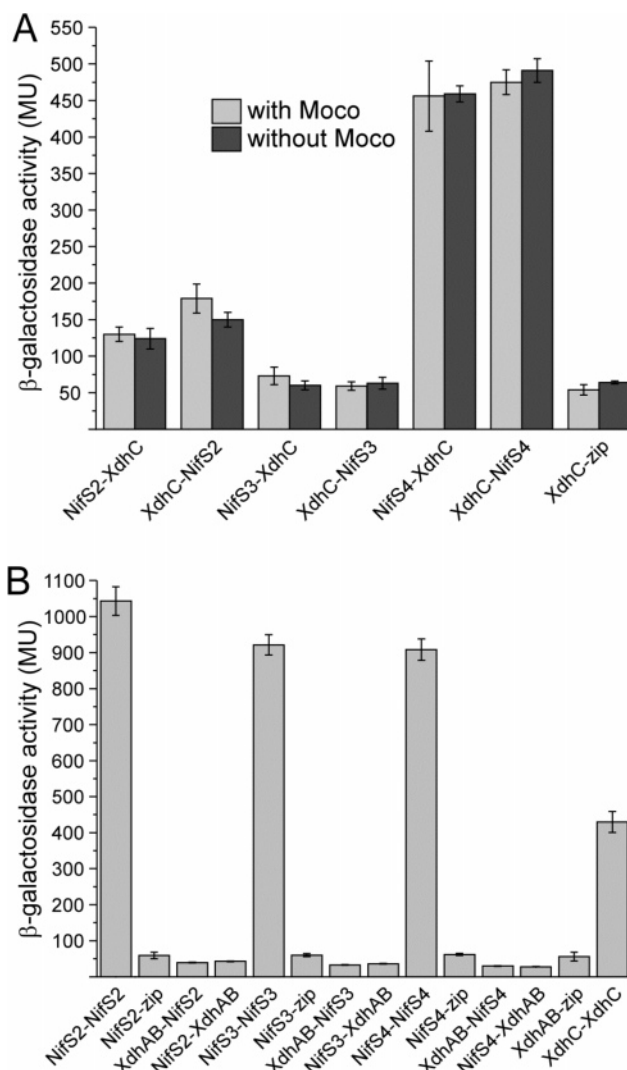


FIGURE 2: Protein–protein interactions between L-cysteine desulfurases and XdhC detected by an *E. coli* two-hybrid approach. Light gray bars represent results from the *E. coli* strain BHT101; dark gray bars represent results obtained in the BHT101moa mutant impaired in Moco biosynthesis. Interaction partners fused to the T18 fragment are listed first and proteins fused to the T25 fragment second. β -Galactosidase activities are expressed in Miller units (MU). (A) Pairwise combinations of L-cysteine desulfurases and XdhC. (B) Direct combinations between XdhAB or XdhC and each L-cysteine desulfurase. As a control for protein multimerization, self-interaction of NifS2, NifS3, or NifS4 was assayed. Background interactions with the leucine zipper were performed with pT18-zip and pT25-zip, but only the results for the pT25-zip interaction are shown.

XdhC interacted specifically with the Moco-containing subunit XdhB of XDH (10). To identify the in vivo protein–protein interactions between NifS2, NifS3, NifS4, and XdhC or XDH, a bacterial two-hybrid system was used, originally described by Karimova et al. (29). Among the pairwise combinations examined, only the combinations of XdhC and NifS4 gave significant values above background (Figure 2A). A weak interaction between XdhC and NifS2 was obtained, showing a β -galactosidase activity twice above background, while no interaction was seen between XdhC and NifS3 (Figure 2A). Also, no β -galactosidase activity above background was identified for XdhAB and NifS2, NifS3, or NifS4 (Figure 2B), showing the specificity of the NifS4–XdhC interaction. In general, background activity is due to an

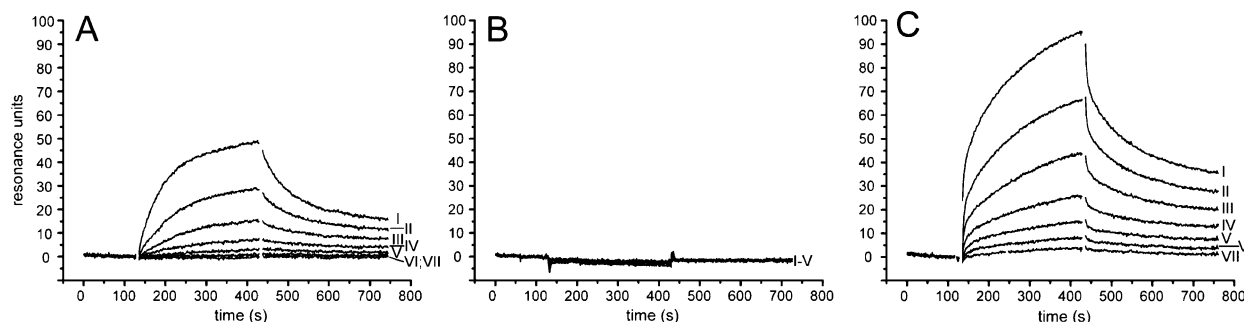


FIGURE 3: Analysis of protein–protein interactions between the purified L-cysteine desulfurases and XdhC by surface plasmon resonance experiments. Biacore sensorgrams of varying concentrations of (A) NifS2- Δ 1–188, (B) NifS3, or (C) NifS4 and immobilized XdhC (570–650 RU) on a CM5 chip. The sensorgram for the control cell (immobilized bovine serum albumin) was subtracted from the sensorgram for the experimental flow cells. Cells were regenerated by injection of 20 mM HCl. L-Cysteine desulfurase concentrations were as follows: 6.4 μ M (I), 3.2 μ M (II), 1.6 μ M (III), 0.8 μ M (IV), 0.4 μ M (V), 0.2 μ M (VI), and 0.1 μ M (VII).

incomplete suppression of the *lacZ* promoter and was obtained by testing the respective fusion proteins with the counterpart fused to the leucine zipper (Figure 2). Negative controls using either pT18-zip or pT25-zip plasmids resulted in the same background values (pT18-zip data not shown). As a control for protein expression, stability, and correct folding, the direct interactions of NifS2, NifS3, NifS4, and XdhC with each other were also analyzed (Figure 2B). The β -galactosidase activities obtained for each interaction pair showed that NifS2, NifS3, NifS4, and XdhC formed dimers/multimers (Figure 2B), with the XdhC dimer giving the lowest values. To compare the influence of the presence of Moco on the XdhC–NifS protein–protein interactions, the interactions were analyzed in parallel in the *E. coli* BHT101 strain and in BHT101*moa*, being devoid of Moco. In general, the same β -galactosidase values were obtained for all tested interactions independent of the availability of Moco in the cell, as shown in Figure 2A. Only the XdhAB and XdhC pairs showed a higher interaction in the absence of Moco using strain BHT101*moa* (data not shown), confirming previous results that only Moco-free XDH interacts with XdhC (10).

To eliminate false negative results and to confirm the *in vivo* interactions identified in the two-hybrid system between XdhC and NifS4, SPR measurements were employed for real time detection of specific interactions using the purified proteins. XdhC was immobilized via amine coupling to a CM5 chip, and successful coupling was confirmed by analysis of the interaction between XdhC and XDH, which has been reported previously (10). The results obtained by SPR confirmed nicely the results of the two-hybrid assay described above, since NifS4 showed the best interaction with immobilized XdhC (Figure 3C). NifS2- Δ 1–188 showed a weaker interaction with XdhC (Figure 3A), and NifS3 did not interact with XdhC (Figure 3B). Global fitting revealed a heterogeneous binding of both proteins. For NifS4 a tight interaction with XdhC was observed, revealing a K_D of 0.64 μ M for the slow dissociating part ($\chi^2 = 1.02$). The interaction for NifS2- Δ 1–188 was less tight, showing a K_D of 13 μ M for the slower dissociating part ($\chi^2 = 0.34$). This clearly shows that the weaker interaction of NifS2 to XdhC previously obtained by the two-hybrid assay is not due to the instability of the N-terminal domain of NifS2.

In Vitro Sulfuration of Moco by L-Cysteine Desulfurases. We showed previously that the *E. coli* L-cysteine desulfurase CsdA is able to sulfurate reduced Moco which is bound to

XdhC (10). Thus, it was of interest to determine whether the *R. capsulatus* L-cysteine desulfurases are able to perform the same reaction. To compare the sulfur transfer efficiencies of NifS2, NifS3, and NifS4 to XdhC, the sulfuration levels of isolated Moco were analyzed subject to the presence or absence of XdhC. Since NifS2, NifS3, and NifS4 showed different k_{cat} values with L-cysteine (Table 2), the L-cysteine desulfurases were persulfurated, and the persulfuration rate was determined for each protein. The proteins showed a persulfuration rate of 54% for NifS2- Δ 1–188, 59% for NifS3, and 77% for NifS4. To compare the L-cysteine desulfurase activities in the following assay, the values for each protein were normalized to a persulfuration grade of 100%. For the *in vitro* formation of the Mo=S ligand of Moco, the persulfurated L-cysteine desulfurases were incubated with excess dioxo Moco extracted from hSO and sodium dithionite either in the absence or in the presence of XdhC. Subsequently, Moco-free apo-XDH was added to the incubation mixtures, and the successful sulfuration of Moco was determined by the reconstitution of XDH activity. As shown in Figure 4, the XDH activities obtained with either NifS2, NifS3, or NifS4 were comparable. As observed previously, XdhC is essential for this reaction, facilitating the sulfuration of Moco when it is protein-bound and stabilizing the sulfurated Moco (10). It has been shown previously that free sulfurated Moco loses the terminal sulfur ligand in solution (10, 33). The XDH activities using the L-cysteine desulfurases are significantly higher than by chemical sulfuration using sodium sulfide as sulfur donor, even when a 3.5 times higher excess of sodium sulfide to persulfurated L-cysteine desulfurase was used.

Further, it was of interest to determine whether the sulfuration of Moco by an L-cysteine desulfurase is more effective when the dioxo form of Moco is bound to XdhC or is already inserted into XDH. In the first set of experiments, isolated Moco was incubated with persulfurated NifS4 in the presence or absence of XdhC prior to its insertion into apo-XDH (Figure 5A). In contrast to the incubation mixtures described above, a 5 times excess of XdhC was used to ensure that free Moco is completely bound to XdhC and that only XdhC-bound Moco and not free Moco is transferred to apo-XDH. In the second set of experiments, Moco was directly inserted into XDH before the addition of either persulfurated NifS4 or sodium sulfide for chemical sulfuration (Figure 5A). After Moco insertion, the XDH activity and the amount of Moco (quantified as form A) were

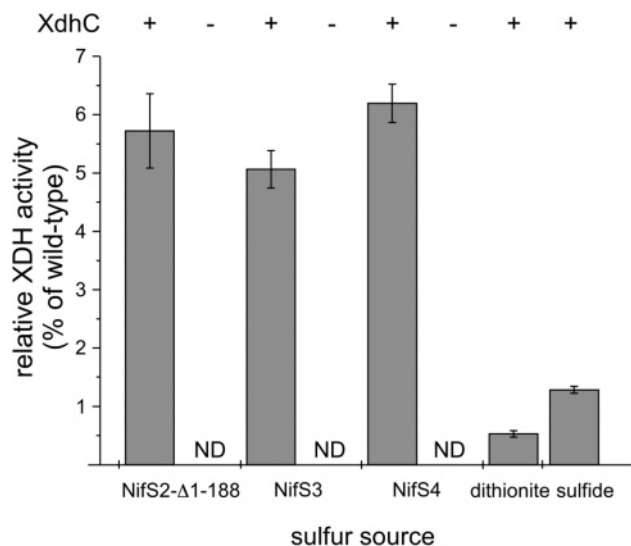


FIGURE 4: In vitro sulfuration of Moco by L-cysteine desulfurases in the presence or absence of XdhC. 20 μ M persulfurated NifS2- Δ 1-188, NifS3, and NifS4, 100 μ M sodium dithionite, and 45 μ M free Moco were mixed in the presence or absence of 2 μ M XdhC and incubated for 1 h at 4 $^{\circ}$ C. Subsequently, 5 μ M apo-XDH was added, and the mixtures were incubated for additional 2 h before XDH activity was determined. For determination of the chemical sulfuration by 100 μ M dithionite and 75 μ M sulfide, samples were incubated without the addition of an L-cysteine desulfurase. The XDH activities were normalized to the determined persulfuration grade of each L-cysteine desulfurase, and the wild-type activity of XDH published previously was set to 100% activity (9). ND, none detectable.

determined. While the Moco saturation of reconstituted XDHs was comparable in all incubation mixtures with values of 7–9% (Figure 5C), the XDH activities differed significantly (Figure 5B). The highest XDH activity was obtained when Moco was sulfurated when it was bound to XdhC and prior to its insertion into apo-XDH (panel I in Figure 5B). When XdhC was omitted from the incubation mixture, no XDH activity was obtained (panel II in Figure 5B). This result is in agreement with previous results, showing that the sulfurated form of Moco loses its sulfur when Moco is free in solution (10, 33). It is also questionable whether free Moco can be sulfurated in solution. When Moco was sulfurated by NifS4 after its insertion into XDH, a 50% lower XDH activity was obtained (panel III in Figure 5B). This sulfuration reaction occurs by formation of free sulfide after cleavage of the persulfide group on NifS4 so that the sulfuration is possible without an interaction between NifS4 and XDH. Exchange of NifS4 by sodium sulfide as direct sulfur donor resulted in a 50% lower XDH activity (panel IV in Figure 5). These results show that Moco sulfuration by an L-cysteine desulfurase is most effective when the cofactor is bound to XdhC. The low XDH activities obtained in this experiment are consistent with a previous report, showing that the maximum of the achievable reconstitution level of XDH with Moco is 15% (10). This reconstitution efficiency is less than the in vitro insertion of Moco described for hSO, where about 30–50% levels could be achieved, depending on the assay conditions (34, 35). We interpreted the lower amounts of Moco insertion into XDH in comparison to hSO with the fact that XDH displays a 2.5 times higher molecular mass (275 kDa) than hSO (~110 kDa), so that the lower levels of in vitro Moco reconstitution might be due to the complexity of the XDH structure and consequently

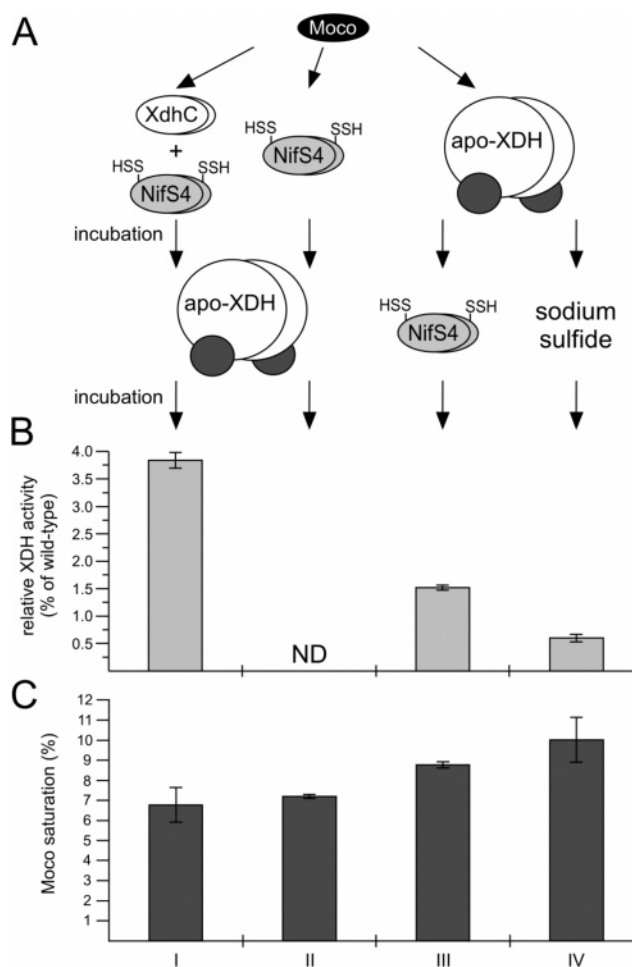


FIGURE 5: In vitro sulfuration of Moco before and after the insertion into the apo-XDH. (A) Schematic representation of the incubation mixtures. (I + II) Mixtures contained 11.6 μ M persulfurated NifS4, 4 μ M dithionite, 2 μ M Moco, and 10 μ M XdhC (I) or no XdhC (II). (III + IV) Mixtures contained 1 μ M apo-XDH, 2 μ M Moco, 4 μ M sodium dithionite, and either 11.6 μ M persulfurated NifS4 (III) or 10 μ M sodium sulfide (IV). (B) The specific activity of the reconstituted XDH is defined as the reduction of 1 μ mol of NAD^+ min^{-1} ($\text{mg of protein}^{-1}$). The XDH activities were normalized to the determined persulfuration grade of NifS4, and the wild-type activity of XDH published previously was set to 100% activity (9). (C) Moco saturation of XDH as determined after conversion to Form A (Experimental Procedures). ND, none detectable.

to a less stable conformation of the Moco-free apo-XDH. In addition, when Moco was sulfurated while bound to XdhC, it remains possible that, due to the in vitro conditions, the Mo=S group gets lost at least to some extent during the insertion reaction into XDH.

DISCUSSION

The crystal structures of several molybdoenzymes revealed that Moco is deeply buried inside the proteins, at the end of a funnel-shaped passage giving access only to the substrate (3, 4, 36, 37). This implied the requirement of specific chaperones for each molybdoenzyme to facilitate the insertion of Moco. For *R. capsulatus* XDH, the XdhC protein has been identified to be involved in the maturation of apo-XDH (10). In prokaryotes, a number of specific chaperones were identified, like TorD for *E. coli* trimethylamine oxide (TMAO) reductase (TorA) or NarJ for *E. coli* nitrate reductase A (NarGHI) (38–40). However, the role of XdhC

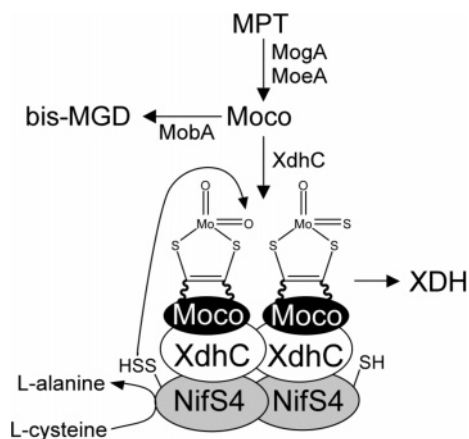


FIGURE 6: Model for the role of NifS4 in sulfuration of Moco bound to XdhC. Moco is produced from MPT, by insertion of the molybdenum atom by aid of MoeA and MogA. Previous results showed that XdhC binds Moco and subsequently inserts it into apo-XDH. The results reported here showed that NifS4 specifically interacts with XdhC and sulfurates bound Moco.

seems to be different from the role of the other chaperones. XdhC represented the first example of a system-specific protein involved in the maturation of a molybdoenzyme, for which Moco binding was identified (10). In contrast, for TorD or NarJ it was rather shown that these proteins stabilize a certain conformation of their target proteins. TorD was shown to interact with TorA to generate a form of the protein competent to accept a bismolybdopterin guanine dinucleotide cofactor (bis-MGD) and to prevent the export of immature TorA (41–43). NarJ is known to bind on two distinct sites of the aponitrate reductase: on the one hand, it facilitates the correct membrane anchoring by avoiding the anchoring of an immature NarGH complex (44), and on the other hand, NarJ allows the Moco insertion through binding to NarG and the Moco biosynthesis proteins (45). For both NarJ and TorD, neither Moco nor bis-MGD binding has been demonstrated to date. Since TorD and NarJ interact with molybdoenzymes that contain the bis-MGD cofactor, their role might be different from the role of XdhC for XDH, binding the MPT form of Moco. It is believed that bis-MGD and Moco biosynthesis are parted at a stage in the cell, after the insertion of the molybdenum atom into MPT (Figure 6). The *E. coli* proteins MogA and MoeA were shown to be involved in the insertion of molybdate into formed MPT (34, 46). At this stage the cofactor has to be divided; one part is inserted into molybdoenzymes binding the MPT form of Moco, and the other part is further modified by involvement of MobA (47), adding an additional nucleotide, and forming the bis-MGD cofactor for enzymes like nitrate reductase or TMAO reductase (48). For enzymes like XDH, the Moco has to be further modified by exchanging one oxo ligand of the Mo center by sulfur, building the equatorial Mo=S ligand. So far, XdhC was shown to protect Moco from oxidation, but a direct role in the sulfuration of Moco has not been demonstrated. Also, a specific protein involved in sulfur transfer to Moco remained unknown in prokaryotes. In contrast, in eukaryotes a number of specific Moco sulfurases were reported that are essential for the activity of XDH and AO by sulfur transfer from their N-terminal NifS-like domain, transferring sulfur from L-cysteine for the sulfuration of Moco (12–14, 17). Further, in plants it was shown that a mutation in the Moco sulfurase is not

complemented by one of the other NifS-like proteins, showing the high specificity of the protein for Moco sulfuration. An important role in recognition of the respective target protein has been designated for the C-terminal domain of the Moco sulfurase. For ABA3 it was suggested that the C-terminal domain coordinates the sulfur transfer from one subunit of ABA3 to one subunit of AO or XDH, enhancing the efficiency of the reaction (18). So far, the binding of Moco has not been reported for the C-terminal domain of Moco sulfurases in eukaryotes. We believe that XdhC, a Moco binding protein, might have a role similar to that of the C-terminal domain of eukaryotic Moco sulfurases; however, no obvious amino acid sequence identities exist between Moco sulfurases and XdhC. Additionally, chaperones involved in binding and/or insertion of Moco seem to be restricted to molybdoenzymes binding bis-MGD or the sulfurated form of Moco. A chaperone seems not to be required for the insertion of dioxo Moco into eukaryotic sulfite oxidase, a protein located in the intermembrane space of mitochondria (49). Here, a protein on the mitochondrial outer membrane was postulated to act as a cofactor source of sulfite oxidase (50). However, this protein has not been further characterized to date, and nothing is known about the mechanism of insertion of dioxo Moco into sulfite oxidase.

To identify the specific L-cysteine desulfurase for the sulfuration of Moco in *R. capsulatus*, we used a direct *E. coli* two-hybrid screen and verified the *in vivo* protein–protein interactions with the purified proteins using SPR measurements. A specific role for the three L-cysteine desulfurases beside NifS, designated NifS2, NifS3, and NifS4, had not been assigned so far. Interposon mutagenesis of the *nifS2*, *nifS3*, and *nifS4* genes showed that *nifS2* strains displayed no particular XDH phenotype and that *nifS3* and *nifS4* are apparently essential for the viability of *R. capsulatus*.²

Our studies identified specific interactions of XdhC with NifS4, displaying a dissociation constant of 0.64 μ M. A significantly weaker interaction was identified between XdhC and NifS2 ($K_D = 13 \mu$ M), while XdhC did not interact with NifS3. Thus, we believe that NifS4 is the specific L-cysteine desulfurase for Moco sulfuration in *R. capsulatus*. However, since interposon mutagenesis of *nifS4* was not successful, the protein appears to have an additional role in another essential sulfur transfer pathway in the cell. A weaker interaction was identified between XdhC and NifS2 by SPR and two-hybrid analyses. However, since interposon mutants in *nifS2* had no influence on XDH activity, we suggest that NifS2 is not involved in the specific sulfuration of Moco in *R. capsulatus* or another protein is able to at least partly compensate for the role of NifS2.

Our *in vitro* studies showed that all L-cysteine desulfurases are able to sulfurate Moco to the same extent. Since this sulfuration can be ascribed to the formation of sulfide after cleavage of the persulfide group, it can be assumed that any protein that releases sulfide is able to sulfurate Moco *in vitro*, an observation which has also been described by Heidenreich et al. (18) for ABA3. However, our results showed that the sulfuration of Moco by an L-cysteine desulfurase is more effective than adding free sulfide, revealing the specificity of the reaction. While by chemical sulfuration with free sulfide both oxo groups of Moco can be replaced by sulfur,

the reaction using an L-cysteine desulfurase has to be more specific, exchanging only the equatorial oxygen by sulfur.

In addition, we addressed the question whether Moco is sulfurated before or after its insertion into XDH. So far it was believed that, in eukaryotes, the sulfuration of Moco occurs after its insertion into AO or XDH. Both the sulfurated and the dioxo form of Moco were identified in AO and XDH in *D. melanogaster* (11), showing that there is no system in eukaryotes ensuring only the insertion of the Mo=S form of Moco into these enzymes. In plants it was believed that, by control of the sulfuration status of these enzymes, the organism is rapidly able to increase XDH and AO activities without the de novo synthesis of these enzymes (18). This implied that eukaryotic Moco sulfurases have a posttranslational regulatory role for enzyme activity. Our studies revealed a different mechanism for Moco sulfuration in prokaryotes. We clearly show that the sulfuration of Moco occurs before its insertion of Moco into XDH, while the cofactor is bound to XdhC. A specific interaction of NifS4 with XdhC was identified, and it was shown that NifS4 does not interact with XDH. In addition, the sulfuration of Moco was more effective when it was bound to XdhC rather than after its insertion into XDH. These results are consistent with previous reports, showing that in an *R. capsulatus* *xdhC* strain XDH contained no Moco, revealing that only the sulfurated form of Moco is specifically inserted into XDH in *R. capsulatus* (7). In addition, it was shown that XdhC stabilizes the sulfurated form of Moco from oxidation (10). The model in Figure 6 summarizes our results, illustrating that, after Mo insertion into MPT, Moco biosynthesis is parted, and dioxo Moco is deducted from further modification to bis-MGD by binding to XdhC. XdhC interacts with NifS4 which specifically exchanges the equatorial oxo ligand of Moco by sulfur. XdhC protects the sulfur ligand of sulfurated Moco from oxidation and specifically inserts the cofactor into the XdhB subunit of XDH. In total, we believe that the XdhC–NifS4 pair in *R. capsulatus* is the counterpart to eukaryotic Moco sulfurases. In eukaryotes both proteins are fused and have a highly specific role for the formation of sulfurated Moco.

ACKNOWLEDGMENT

We thank K. V. Rajagopalan (Duke University) for providing pTG818, Manfred Nimtz (Braunschweig) for performing MALDI MS experiments, and Bernd Masepohl (Bochum) for providing plasmids containing the coding regions of *nifS2*, *nifS3*, and *nifS4* and for providing details to describe unpublished data about the construction of *nifS* mutants in *R. capsulatus*.

APPENDIX

For the construction of *R. capsulatus* *nifS3* and *nifS4* mutants, various plasmids were constructed for plasmid integration and interposon mutagenesis. So far, all attempts to obtain mutants in *nifS3* or *nifS4* failed, pointing toward an essential function of both genes, e.g., in iron–sulfur cluster biosynthesis. Bernd Masepohl agreed to describe the data as unpublished results in the text.

SUPPORTING INFORMATION AVAILABLE

An amino acid sequence alignment for the *R. capsulatus* L-cysteine desulfurases NifS2, NifS3, and NifS4 in com-

parison to *E. coli* IscS, CsdB, and CsdA (Figure S1). This material is available free of charge via the Internet at <http://pubs.acs.org>.

REFERENCES

- Hille, R. (1996) The mononuclear molybdenum enzymes, *Chem. Rev.* 96, 2757–2816.
- Hille, R., and Sprecher, H. (1987) On the mechanism of action of xanthine oxidase. Evidence in support of an oxo transfer mechanism in the molybdenum-containing hydroxylases, *J. Biol. Chem.* 262, 10914–10917.
- Enroth, C., Eger, B. T., Okamoto, K., Nishino, T., Nishino, T., and Pai, E. F. (2000) Crystal structures of bovine milk xanthine dehydrogenase and xanthine oxidase: structure-based mechanism of conversion, *Proc. Natl. Acad. Sci. U.S.A.* 97, 10723–10728.
- Truglio, J. J., Theis, K., Leimkühler, S., Rappa, R., Rajagopalan, K. V., and Kisker, C. (2002) Crystal structures of the active and alloxanthine-inhibited forms of xanthine dehydrogenase from *Rhodobacter capsulatus*, *Structure (Cambridge)* 10, 115–125.
- Gutteridge, S., Tanner, S. J., and Bray, R. C. (1978) Comparison of the molybdenum centres of native and desulpho xanthine oxidase. The nature of the cyanide-labile sulphur atom and the nature of the proton-accepting group, *Biochem. J.* 175, 887–897.
- Massey, V., and Edmondson, D. (1970) On the mechanism of inactivation of xanthine oxidase by cyanide, *J. Biol. Chem.* 245, 6595–6598.
- Leimkühler, S., and Klipp, W. (1999) Role of XDHc in molybdenum cofactor insertion into xanthine dehydrogenase of *Rhodobacter capsulatus*, *J. Bacteriol.* 181, 2745–2751.
- Leimkühler, S., Hodson, R., George, G. N., and Rajagopalan, K. V. (2003) Recombinant *Rhodobacter capsulatus* xanthine dehydrogenase, a useful model system for the characterization of protein variants leading to xanthinuria I in humans, *J. Biol. Chem.* 278, 20802–20811.
- Leimkühler, S., Stockert, A. L., Igarashi, K., Nishino, T., and Hille, R. (2004) The role of active site glutamate residues in catalysis of *Rhodobacter capsulatus* xanthine dehydrogenase, *J. Biol. Chem.* 279, 40437–40444.
- Neumann, M., Schulte, M., Junemann, N., Stocklein, W., and Leimkühler, S. (2006) *Rhodobacter capsulatus* XdhC is involved in molybdenum cofactor binding and insertion into xanthine dehydrogenase, *J. Biol. Chem.* 281, 15701–15708.
- Wahl, R. C., Warner, C. K., Finnerty, V., and Rajagopalan, K. V. (1982) *Drosophila melanogaster* *ma-l* mutants are defective in the sulfuration of desulfo Mo hydroxylases, *J. Biol. Chem.* 257, 3958–3962.
- Amrani, L., Primus, J., Glatigny, A., Arcangeli, L., Scazzocchio, C., and Finnerty, V. (2000) Comparison of the sequences of the *Aspergillus nidulans* *hxB* and *Drosophila melanogaster* *ma-l* genes with *nifS* from *Azotobacter vinelandii* suggests a mechanism for the insertion of the terminal sulphur atom in the molybdopterin cofactor, *Mol. Microbiol.* 38, 114–125.
- Ichida, K., Matsumura, T., Sakuma, R., Hosoya, T., and Nishino, T. (2001) Mutation of human molybdenum cofactor sulfurase gene is responsible for classical xanthinuria type II, *Biochem. Biophys. Res. Commun.* 282, 1194–1200.
- Watanabe, T., Ihara, N., Itoh, T., Fujita, T., and Sugimoto, Y. (2000) Deletion mutation in *Drosophila* *ma-l* homologous, putative molybdopterin cofactor sulfurase gene is associated with bovine xanthinuria type II, *J. Biol. Chem.* 275, 21789–21792.
- Amrani, L., Cecchetto, G., Scazzocchio, C., and Glatigny, A. (1999) The *hxB* gene, necessary for the post-translational activation of purine hydroxylases in *Aspergillus nidulans*, is independently controlled by the purine utilization and the nicotinate utilization transcriptional activating systems, *Mol. Microbiol.* 31, 1065–1073.
- Leydecker, M. T., Moureaux, T., Kraepiel, Y., Schnorr, K., and Caboche, M. (1995) Molybdenum cofactor mutants, specifically impaired in xanthine dehydrogenase activity and abscisic acid biosynthesis, simultaneously overexpress nitrate reductase, *Plant Physiol.* 107, 1427–1431.
- Bittner, F., Oreb, M., and Mendel, R. R. (2001) ABA3 is a molybdenum cofactor sulfurase required for activation of aldehyde oxidase and xanthine dehydrogenase in *Arabidopsis thaliana*, *J. Biol. Chem.* 276, 40381–40384.
- Heidenreich, T., Wollers, S., Mendel, R. R., and Bittner, F. (2005) Characterization of the NifS-like domain of ABA3 from *Arabi-*

- dopsis thaliana* provides insight into the mechanism of molybdenum cofactor sulfuration, *J. Biol. Chem.* 280, 4213–4218.
19. Sagi, M., Scazzocchio, C., and Fluhr, R. (2002) The absence of molybdenum cofactor sulfuration is the primary cause of the flacca phenotype in tomato plants, *Plant J.* 31, 305–317.
 20. Zheng, L., White, R. H., Cash, V. L., and Dean, D. R. (1994) Mechanism for the desulfurization of L-cysteine catalyzed by the *nifS* gene product, *Biochemistry* 33, 4714–4720.
 21. Mihara, H., Kurihara, T., Yoshimura, T., Soda, K., and Esaki, N. (1997) Cysteine sulfinate desulfinase, a NIFS-like protein of *Escherichia coli* with selenocysteine lyase and cysteine desulfurase activities. Gene cloning, purification, and characterization of a novel pyridoxal enzyme, *J. Biol. Chem.* 272, 22417–22424.
 22. Masepohl, B., Angermüller, S., Hennecke, S., Hubner, P., Moreno-Vivian, C., and Klipp, W. (1993) Nucleotide sequence and genetic analysis of the *Rhodobacter capsulatus* ORF6-*nifUI* SVW gene region: possible role of NifW in homocitrate processing, *Mol. Gen. Genet.* 238, 369–382.
 23. Johnson, M. E., and Rajagopalan, K. V. (1987) Involvement of chlA, E, M, and N loci in *Escherichia coli* molybdopterin biosynthesis, *J. Bacteriol.* 169, 117–125.
 24. Temple, C. A., Graf, T. N., and Rajagopalan, K. V. (2000) Optimization of expression of human sulfite oxidase and its molybdenum domain, *Arch. Biochem. Biophys.* 383, 281–287.
 25. Karimova, G., Ullmann, A., and Ladant, D. (2000) A bacterial two-hybrid system that exploits a cAMP signaling cascade in *Escherichia coli*, *Methods Enzymol.* 328, 59–73.
 26. Magalon, A., Frixon, C., Pommier, J., Giordano, G., and Blasco, F. (2002) In vivo interactions between gene products involved in the final stages of molybdenum cofactor biosynthesis in *Escherichia coli*, *J. Biol. Chem.* 277, 48199–48204.
 27. Zheng, L., White, R. H., Cash, V. L., Jack, R. F., and Dean, D. R. (1993) Cysteine desulfurase activity indicates a role for NIFS in metallocluster biosynthesis, *Proc. Natl. Acad. Sci. U.S.A.* 90, 2754–2758.
 28. Urbina, H. D., Silberg, J. J., Hoff, K. G., and Vickery, L. E. (2001) Transfer of sulfur from IscS to IscU during Fe/S cluster assembly, *J. Biol. Chem.* 276, 44521–44526.
 29. Karimova, G., Pidoux, J., Ullmann, A., and Ladant, D. (1998) A bacterial two-hybrid system based on a reconstituted signal transduction pathway, *Proc. Natl. Acad. Sci. U.S.A.* 95, 5752–5756.
 30. Miller, J. H. (1972) *Experiments in Molecular Genetics*, Cold Spring Harbor Laboratory Press, Cold Spring Harbor, NY.
 31. Masepohl, B., Führer, F., and Klipp, W. (2001) Genetic analysis of a *Rhodobacter capsulatus* gene region involved in utilization of taurine as a sulfur source, *FEMS Microbiol. Lett.* 205, 105–111.
 32. Leimkühler, S., Kern, M., Solomon, P. S., McEwan, A. G., Schwarz, G., Mendel, R. R., and Klipp, W. (1998) Xanthine dehydrogenase from the phototrophic purple bacterium *Rhodobacter capsulatus* is more similar to its eukaryotic counterparts than to prokaryotic molybdenum enzymes, *Mol. Microbiol.* 27, 853–869.
 33. Wahl, R. C., Hageman, R. V., and Rajagopalan, K. V. (1984) The relationship of Mo, molybdopterin, and the cyanolyzable sulfur in the Mo cofactor, *Arch. Biochem. Biophys.* 230, 264–273.
 34. Nichols, J. D., and Rajagopalan, K. V. (2005) In vitro molybdenum ligation to molybdopterin using purified components, *J. Biol. Chem.* 280, 7817–7822.
 35. Leimkühler, S., and Rajagopalan, K. V. (2001) In vitro incorporation of nascent molybdenum cofactor into human sulfite oxidase, *J. Biol. Chem.* 276, 1837–1844.
 36. Kisker, C., Schindelin, H., Pacheco, A., Wehbi, W. A., Garrett, R. M., Rajagopalan, K. V., Enemark, J. H., and Rees, D. C. (1997) Molecular basis of sulfite oxidase deficiency from the structure of sulfite oxidase, *Cell* 91, 973–983.
 37. Chan, M. K., Mukund, S., Kletzin, A., Adams, M. W., and Rees, D. C. (1995) Structure of a hyperthermophilic tungstopterin enzyme, aldehyde ferredoxin oxidoreductase, *Science* 267, 1463–1469.
 38. Blasco, F., Dos Santos, J. P., Magalon, A., Frixon, C., Guigliarelli, B., Santini, C. L., and Giordano, G. (1998) NarJ is a specific chaperone required for molybdenum cofactor assembly in nitrate reductase A of *Escherichia coli*, *Mol. Microbiol.* 28, 435–447.
 39. Ilbert, M., Mejean, V., Giudici-Orticoni, M. T., Samama, J. P., and Iobbi-Nivol, C. (2003) Involvement of a mate chaperone (TorD) in the maturation pathway of molybdoenzyme TorA, *J. Biol. Chem.* 278, 28787–28792.
 40. Tranier, S., Mortier-Barriere, I., Ilbert, M., Birck, C., Iobbi-Nivol, C., Mejean, V., and Samama, J. P. (2002) Characterization and multiple molecular forms of TorD from *Shewanella massilia*, the putative chaperone of the molybdoenzyme TorA, *Protein Sci.* 11, 2148–2157.
 41. Genest, O., Ilbert, M., Mejean, V., and Iobbi-Nivol, C. (2005) TorD, an essential chaperone for TorA molybdoenzyme maturation at high temperature, *J. Biol. Chem.* 280, 15644–15648.
 42. Oresnik, I. J., Ladner, C. L., and Turner, R. J. (2001) Identification of a twin-arginine leader-binding protein, *Mol. Microbiol.* 40, 323–331.
 43. Jack, R. L., Buchanan, G., Dubini, A., Hatzixanthis, K., Palmer, T., and Sargent, F. (2004) Coordinating assembly and export of complex bacterial proteins, *EMBO J.* 23, 3962–3972.
 44. Vergnes, A., Pommier, J., Toci, R., Blasco, F., Giordano, G., and Magalon, A. (2005) NarJ chaperone binds on two distinct sites of the aponitrate reductase of *Escherichia coli* to coordinate molybdenum cofactor insertion and assembly, *J. Biol. Chem.*
 45. Vergnes, A., Gouffi-Belhabich, K., Blasco, F., Giordano, G., and Magalon, A. (2004) Involvement of the molybdenum cofactor biosynthetic machinery in the maturation of the *Escherichia coli* nitrate reductase A, *J. Biol. Chem.* 279, 41398–41403.
 46. Nichols, J., and Rajagopalan, K. V. (2002) *Escherichia coli* MoeA and MogA. Function in metal incorporation step of molybdenum cofactor biosynthesis, *J. Biol. Chem.* 277, 24995–25000.
 47. Palmer, T., Santini, C. L., Iobbi-Nivol, C., Eaves, D. J., Boxer, D. H., and Giordano, G. (1996) Involvement of the narJ and mob gene products in distinct steps in the biosynthesis of the molybdoenzyme nitrate reductase in *Escherichia coli*, *Mol. Microbiol.* 20, 875–884.
 48. Temple, C. A., and Rajagopalan, K. V. (2000) Mechanism of assembly of the bis(molybdopterin guanine dinucleotide)molybdenum cofactor in *Rhodobacter sphaeroides* dimethyl sulfoxide reductase, *J. Biol. Chem.* 275, 40202–40210.
 49. Cohen, H. J., Betcher-Lange, S., Kessler, D. L., and Rajagopalan, K. V. (1972) Hepatic sulfite oxidase. Congruency in mitochondria of prosthetic groups and activity, *J. Biol. Chem.* 247, 7759–7766.
 50. Johnson, J. L., Jones, H. P., and Rajagopalan, K. V. (1977) In vitro reconstitution of demolybdosulfite oxidase by a molybdenum cofactor from rat liver and other sources, *J. Biol. Chem.* 252, 4994–5003.